Journal Name

ARTICLE

Assessing Structure and Stability of Polymer/Lithium-Metal Interfaces from First-Principles Calculations

Received 00th January 20xx,

Accepted 00th January 20xx

DOI: 10.1039/x0xx00000x

www.rsc.org/

Mahsa Ebadi,[a] Cleber Marchiori,[b] Jonas Mindemark,[a] Daniel Brandell,[a*] C. Moyses Araujo[b*]

Solid polymer electrolytes (SPEs) are promising candiates for Li metal battery applications, but the interface between these two categories of materials has so far been studied only to a limited degree. A better understanding of interfacial phenomena, primarily polymer degradation, is essential for improving battery performance. The aim of this study is to get insights into atomistic surface interaction and early stages of solid electrolyte interphase formation between ionically conductive SPE host polymers and the Li metal electrode. A range of SPE candidates are studied, representative of major host material classes: polyethers, polyalchohols, polyesters, polycarbonates, polyamines and polynitriles. Density functional theory (DFT) calculations are carried out to study the stability and the electronic structure of such polymer/Li interfaces. The adsorption energies indicated a stronger adhesion to Li metal of polymers with ester/carbonate and nitrile functional groups. Together with a higher charge redistribution, a higher reactivity of these polymers is predicted as compared to the other electrolyte hosts. Products such as alkoxides and CO are obtained from the degradation of ester- and carbonate-based polymers by AIMD simulations, in agreement with experimental studies. Analogous to low-molecular-weight organic carbonates, decomposition pathways through $C_{carbonyl}$–$O_{ethereal}$ and $C_{ethereal}$–$O_{ethereal}$ bond cleavage can be assumed, with carbonate-containing fragments being thermodynamically favorable.

[a] *Department of Chemistry - Ångström Laboratory, Uppsala University, Box 538, 75121 Uppsala, Sweden*
[b] *Materials Theory Division, Department of Physics and Astronomy, Uppsala University, Box 516, 75120 Uppsala, Sweden*
**Corresponding authors*: moyses.araujo@physics.uu.se and daniel.brandell@kemi.uu.se

1. Introduction

Solid polymer electrolytes (SPEs) constitute a promising class of electrolyte materials for applications together with Li metal in all-solid-state batteries. The main advantages of these electrolytes as compared to their conventional liquid counterparts are better battery safety and appealing mechanical properties in terms of both strength and flexibility, which render them functional with the otherwise problematic Li metal electrode.[1] SPE research dates back to the initial observations of Li ion conduction in poly(ethylene oxide) (PEO) during the 1970s.[2,3] Although significant improvements have been made over the years, there still exist some significant hurdles to overcome for large-scale realisation of SPEs in Li batteries. Not least is the low bulk ionic conductivity at ambient temperature problematic, but the chemical and electrochemical compatibility at the electrode–electrolyte interface also raises concerns.[1,4]

PEO and other polyethers have been commonly applied as SPEs in Li-metal batteries (LMBs) since Armand and co-workers explored PEO for this purpose.[5] The ionic conductivity of PEO-based electrolytes is low below 60 °C due to the high crystallinity, while the mechanical stability of the polymer is significantly decreased at higher temperatures.[6,7] Strategies to overcome these problems include for example cross-linking of the polymers and using plasticising Li salts.[1,6]

Other host materials than PEO have also been investigated over the years, and recently experienced somewhat of a renaissance.[7] One type of such 'alternative' polymer hosts is polycarbonates. Important examples in this group are poly(ethylene carbonate) (PEC) and poly(trimethylene carbonate) (PTMC), whose versatile chemistry involving controlled ring-opening polymerisation also allows for facile chemical functionalisation.[8–12] Co-polymers between PTMC and the polyester poly(ε-caprolactone) (PCL) have also generated SPEs with sufficient conductivity to enable battery operation at ambient temperature conditions.[13] Moreover, polyalcohols such as poly(vinyl alcohol) (PVA), polyamines and polynitriles have also been explored as ion-coordinating macromolecular solvents for Li-battery SPEs.[7]

Apart from bulk SPEs, ionically conductive polymers have also been used as thin-film coating layers on Li-metal electrodes, where they can protect the electrode from detrimental interactions with the liquid

electrolyte.[14–16] Here, the polymer coating chemically and electrochemically stabilises the reactive metal surface. Adhesion to the Li electrode is, in this context, decisive, since the polymer would otherwise detach and/or dissolve into the electrolyte.

Besides the large number of experimental studies on SPE materials over the years, there also exists a rich literature on computational studies of this category of materials. Generally, the structure and complexation of ions in the macromolecular solvents have been studied by *ab initio* and density functional theory (DFT) calculations, while transport properties have been investigated through molecular dynamics (MD) simulations.[17–19] These studies are – perhaps even more than the experimental counterparts – dominated by PEO-based materials, and only a limited number of examples treat other polymer host SPEs computationally.[19–21]

Moreover, while the bulk properties of PEO-based SPEs have been comparatively extensively studied using these computational approaches, the interfaces between SPEs and different battery electrodes is yet largely unexplored. Still, these interfaces are what will ultimately control important battery properties such as power performance, capacity degradation and battery ageing. While recent years have seen several first-principles studies of the interface between ceramic electrolytes and various electrodes,[22–31] the corresponding research area for SPEs is virtually unexplored and little is known of how different polymer hosts adhere to and interact with the Li-battery electrodes. In a few examples of classical MD simulations, covering V_2O_5/PEO,[32] TiO_2/PEO[33] and Li-metal/PEO–LiTFSI interfaces,[34] it has been seen that the electrode surface significantly influences polymer structure and density in the interface region, leading to a redistribution of salt and a changed polymer–salt coordination chemistry. The decisive reactivity of the polymer with Li metal has, however, not been possible to study with these classical force field-based methods.

Experimental characterisation of polymer physics and chemistry in the battery system, and the Solid Electrolyte Interphase (SEI) layers formed as a result of electrolyte decomposition reactions, is technically difficult due to the strong adhesion of the polymer to the electrode during battery operation, thereby rendering conventional ex-situ measurements complicated to perform.[35,36] A deeper knowledge at the

atomic-scale level is, however, still required regarding the polymer electrolyte and electrode interface for better understanding of this type of battery cells. For this purpose, DFT and ab-initio MD (AIMD) simulations are here employed to investigate the interface between a range of polymeric SPE host systems and a Li metal surface. These represent realistic LMB systems, and have been extensively employed in SPE research. Several polymers host – PEO, PVA, PEC, PTMC, PCL, polyethylenimine (PEI) and polyacrylonitrile (PAN) – are chosen for investigations of their electronic structures, reactivity and adhesion to the Li metal surface. This renders insights regarding both polymer stability and ionic transport over the crucial electrode/electrolyte interface, especially for the formation of the 'inner' SEI layer in SPE-based solid-state batteries, and for thin-film polymer coatings of the Li metal electrode.

2. Computational details

The main calculations in this work have been performed within the DFT framework and using the projector augmented wave (PAW) method[37,38] as implemented in the Vienna ab initio Simulation Package (VASP).[39] The generalised gradient approximation (GGA) of Perdew, Burke, and Ernzerhof (PBE)[40] was used as the exchange-correlation functional. The plane-wave cut-off was set to 550 eV for all systems in the study. The Brillouin zone integrations for the cells containing polymers adsorbed on the Li metal surface were computed with 3 × 3 × 1 Monkhorst and Pack k-point mesh.[41,42] Gaussian smearing with a width of 0.1 eV was used. In order to include the van der Waals (vdW) correction, the DFT-D3 method was considered, which has been reported as a reasonable choice considering both the computational efficiency and the correction of the adsorption energies of molecules interacting with a metal surface.[43,44]

In order to investigate the influence of the oligomers length on their energetics, a set of benchmark calculations were performed on a molecular level. Gaussian09 package[45] was employed for this purpose since this is a suitable tool for molecular calculations. Oligomers consisting of 1 up to 6 units were fully optimized at M06/6-31G(d)[46–51] level of theory to evaluate the dependence of the frontier orbital energy with the chain length (results shown in Fig. S1). Moreover, total density of states (DOS) of some oligomers (with 3, 5 and 6 monomeric units) were computed, using also DFT/PAW in VASP, in order to investigate the

dependence of the electronic structure on the length of the polymers (see results in Fig. S2). The free polymer chains were modelled in a vacuum box, big enough to avoid periodic image interactions. The Brillouin zone integration was considered at gamma point for the free polymers. These additional calculations were carried out to further validate the oligomer models used in the calculations of the metal-polymer interactions.

Oligomers with three monomeric units were considered for the rest of this study and the random rotor search method in the Avogadro software[52] was applied to obtain the initial conformer of the polymer chains. The oligomers were adsorbed on a Li (100) slab with 5 layers thickness and 36 Li atoms per layer, following our previous study.[44] The supercell was relaxed while keeping the two bottom layers of the slab fixed. Geometry optimisations of the supercells including polymers and Li metal slab were carried out within the convergence criterion of 10^{-4} and 10^{-3} for electronic self-consistent iteration and ionic relaxation, respectively. To improve the description of the Li metal/polymer interface, we have also considered solvation effects using the implicit solvent model as implemented in VASPsol code.[53] The dielectric constants were set to 7 and 37.7 corresponding to PEO polymer electrolyte[54] and acetonitrile[55], respectively. The former is a typical value for the polymeric environment while the latter has been used to estimate the salt effect, which tends to increase the dielectric constant of the polymers. The cut-off charge density was set to 2.5 x 10^{-4} $Å^{-3}$ and the contribution of cavitation has been neglected.[44,55] Partial DOS were calculated using Gaussian smearing with a width of 0.1 and a 7 x 7 x 1 Monkhorst–Pack k-point mesh for better accuracy.

To further investigate the reactivity of the polymeric compounds with the Li metal surface, AIMD simulations using the Verlet integration algorithm were carried out for 15 ps simulation time. We have used the Born-Oppenheimer approach as implemented in VASP. In these simulations, the thickness of the Li metal slab was set to three layers while keeping the bottom layer fixed. Velocities were rescaled every 4 steps to equilibrate the system at a temperature of 400 K and 600 K. Tritium masses replaced hydrogen masses in order to allow a time step of 1 fs. A convergence criterion of 10^{-5} eV was applied for the electronic self-consistency.

3. Results and discussion

3.1 Polymeric compounds

Several potential polymers which are interesting as candidate host materials for LMB applications were selected and studied in this work; Fig. 1 shows the seven different polymers included. All the oligomers displayed a very weak dependence of the frontier orbitals energy on the variation of the chain length (Fig. S1). Since these polymers are non-conjugated materials, the polymeric backbones are built mainly by sp^3 carbons with the electronic structure displaying a more localized character and then such a weak dependence on the oligomer size. These results are also corroborated by the computed total DOS shown in Fig. S2. Therefore, the length of each oligomer was set to three units in order to fit to the 6×6 atom surface area of the Li slab.

Alkyl end groups (generally $–CH_3$) were used as terminal groups since their interactions with the Li-metal surface should be limited as compared to alternatives (see Fig. 1). Polymers can generally adopt different conformations both in bulk and on surfaces. Both randomly generated coils and linear conformers were therefore considered to compare their respective energies. The calculated energy difference for the two conformers was, however, not significant (around 0.1–0.2 eV) at this limited chain length for any of the investigated polymers, and the random coil conformers were selected for the rest of the study.

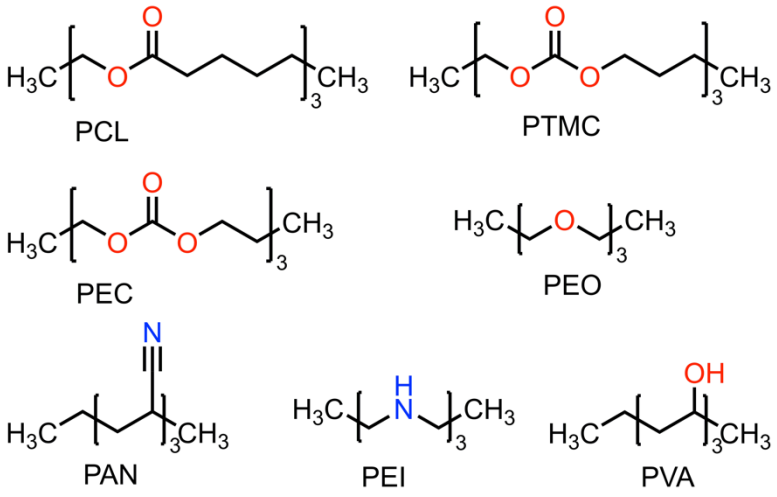

Fig. 1. Structures of the different oligomer fragments investigated, including their terminal groups.

3.2 Polymers adsorbed on the Li metal surface

All oligomers were individually placed on the Li (100) surface to investigate their interactions when in contact with Li metal. The optimised structures of these systems are shown in Fig. 2. It is anticipated that the interactions with Li metal via groups containing polar atoms (N or O) is strong due to their high electronegativity. In order to see the effects of the interactions with the surface on the structures of the polymers, the calculated bond distances of the functional groups in each polymer before and after the adsorption are presented in Table 1.

Fig. 2a shows the adsorbed PEO oligomer. As can be seen, the Li atoms of the surface move towards the O atoms following atomic relaxations. The average C–O bond distance in PEO before adsorption is around 1.42 Å (in good agreement with the reported experimental value for C–O in ethers)[56] while the C–O bond elongates to around 1.44–1.45 Å after adsorption. PVA adsorbed at the surface is shown in Fig. 2b. The Li atoms are interacting with O in the oligomer in a similar way as for PEO. The average C–O bond distances in PVA before and after the adsorption are around 1.44–1.45 Å and 1.47 Å, respectively. PEC, the carbonate analogue of PEO, shown in Fig. 2c, has two different C–O bonds; ethereal and carbonyl. It is the carbonyl oxygen that binds directly to the metal surface. The carbonyl and the ethereal bond lengths upon adsorption on the surface slightly elongates and decreases, respectively. Similar patterns have been reported for changes in the bond lengths of organic carbonate solvents binding to a Li metal surface.[44]

A C–N bond enhancement to around 0.02 Å is obtained upon adsorption for PEI, an analogue of PEO having NH instead of O atoms (Fig. 2d). PCL (Fig. 2e) has ester functional groups, and therefore has carbonyl and ethereal C=O and C–O bonds. Similar elongation and reduction, respectively, as in PEC are obtained for the carbonyl and ethereal C–O in this oligomer upon adsorption on the surface. In Fig. 2(f), the adsorbed PTMC is presented, and as in PEC and PCL the C–O ethereal and carbonyl bond distances are reduced and increased, respectively, upon adsorption. Here, it is also primarily the carbonyl oxygens which interact directly with the metal surface. It can be seen in Fig. 2g that the optimised structure of the adsorbed PAN

has undergone a ring formation through a bond formation between two C atoms of neighbouring nitrile groups. The formed C–C bond distance is 1.44 Å, which is intermediate between common single and double C–C bond distances. The triple bond distance in the nitrile group is 1.16 Å, which after formation of the ring becomes 1.38 Å, and therefore has been transformed to a C=N (double) bond. The nitrile group is indeed a strongly electron-withdrawing group, and charge redistribution can therefore occur between the nitrile group and the surface, which can lead to changes in the hybridisation of this functional group during relaxation and interactions with the Li atoms in the metal surface.

The adsorption energies of the molecules on the Li metal surface are calculated as:

$$E_{\text{ads}} = E_{\text{Polymer close to Li (100)}} - E_{\text{Polymer far from Li (100)}} \qquad (1)$$

where $E_{\text{Polymer close to Li (100)}}$ and $E_{\text{Polymer far from Li (100)}}$ are the total energies of the system containing the polymer interacting with the Li metal surface and the system with the polymer locating in the middle of vacuum region (around 8–10 Å far from the surface), respectively. The results for the adsorption energies in the vacuum, and including solvation effect (PEO and acetonitrile) are shown in Fig. 3. More negative adsorption energies indicate stronger adhesion to the surface. As can be seen in Fig. 3, the trend obtained for the three different cases are very similar with small energy differences among these models. Therefore, the vacuum model has been used for the rest of this study.

Interestingly, the adsorption energy of PAN (−6.88 eV) is quite different from the other molecules. The strongly electron-withdrawing characteristics of the nitrile group is likely to be the reason for the stronger interaction of PAN with the Li metal surface.

The second-strongest interaction on the Li metal surface is seen for PEC (−3.44 eV), but the difference among the adsorption energies for PEC and the other oligomers is not as high as for PAN. The carbonate group is also expected to have a strong interaction with the Li atoms on the surface due to the polarity of the carbonyl C=O bond. The order of the absolute value of the calculated adsorption energies among the ester/carbonate containing polymers is PEC (−3.44 eV) > PTMC (−3.02 eV) > PCL (−2.49 eV). This could be considered somewhat surprising, since the carbonate group in PEC and PTMC possess one extra ethereal electron-withdrawing oxygen as compared to the ester group in PCL, and should therefore be somewhat

less polar. For PEC and PTMC, however, the hybridisation of one carbon of the carbonyl group changes from sp^2- to sp^3-like due to strong interactions with the Li atoms of the surface, which better explain their stronger adsorption. The lower adsorption energies of PTMC and PCL can also be related to geometric effects due to the longer monomeric units as compared to the PEC molecule, which can make it more difficult to obtain an energetically favourable arrangement with the Li atoms on the metal surface.

PVA and PEO have quite similar adsorption energies, which is −0.03 eV more negative for PEO (−1.48 eV) than PVA (−1.45 eV). The lowest adsorption energies belong to PEI trimer (−1.19 eV). Thus, PEI displays the weakest adsorption capability.

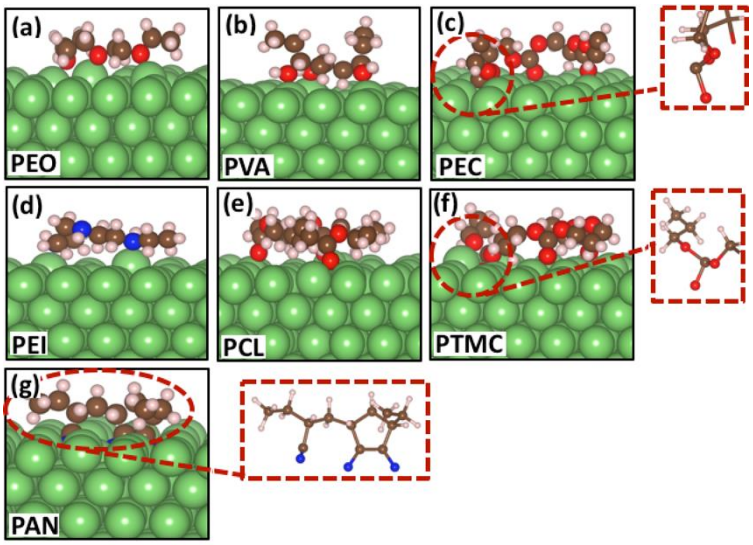

Fig. 2. Top views of optimised structures of (a) PEO (b) PVA (c) PEC (d) PEI (e) PCL (f) PTMC (g) PAN oligomers on a Li (100) slab. Green, red, dark blue, brown and light pink colours denote the Li, O, N, C and H atoms, respectively.

Table 1. C–N and C–O bond lengths (Å) in the oligomers before and after adsorption on the Li (100) surface.

Oligomers	C–N/C–O bond lengths	
	Before adsorption	After adsorption
PEO	1.42	1.44-1.45
PVA	1.44–1.45	1.47
PEC	1.21[a]	1.23–1.24[a]
	1.35–1.36[b]	1.33–1.34[b]
PEI	1-46	1.48
PCL	1.22[a]	1.25[a]
	1.36[b]	1.34[b]
PTMC	1.22[a]	1.25[a]

	1.35[b]	1.33[b]
PAN	1.16	1.3
		1.38[c]

[a] The C–O bond distance of the carbonyl part. [b] The C–O bond distance of the ethereal part. [c] The bond distances of deformed C–N.

The adhesion of polymers to the surface can be considered as a key factor in understanding the electrolyte/electrode stability in the battery system, and certainly a decisive factor for polymeric coatings. Nevertheless, adhesion can be interpreted in two different ways. On the one hand, a stronger adhesion of the polymeric molecules on the surface can generate a more stable interface between the two materials, since they are strongly bonded together. This can also facilitate ion transport over the electrode/electrolyte interface, thereby resulting in a better power capability through increased surface 'wetting'. On the other hand, strong adhesion of a polymer to the Li-metal surface is indicative of stronger interactions between the two materials, which can lead to a reduction of the molecule on the surface of the metal. Polymers with a fairly strong adhesion, but which do not decompose, would in this context constitute a functional compromise. It should, however, be kept in mind that other factors and components than the polymer chemistry itself also likely play important roles for the overall interactions of SPEs with Li metal, not least the presence of electrolyte salt.

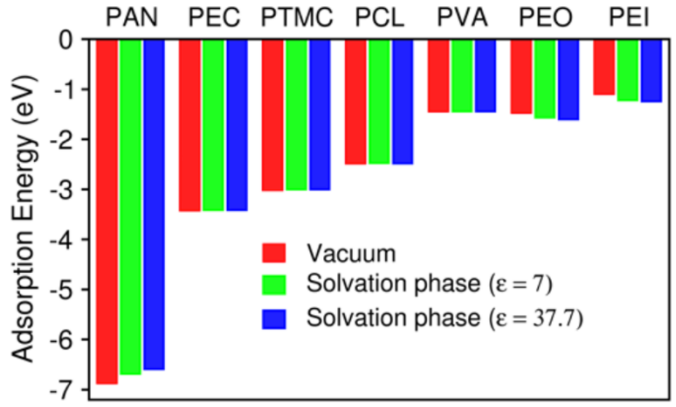

Fig. 3. Adsorption energies of PAN, PTMC, PCL, PEC, PEI, PEO and PVA at the Li (100) surface, in the vacuum, implicit solvent model with dielectric constant 7 and dielectric constant 37.7, respectively.

To get better insight into how the charge distribution changes upon adsorption of the polymers on the metal surface, the 3D charge density difference (CCD) has been computed:

$$\Delta\rho = \rho_{\text{Polymer@Li (100)}} - \rho_{\text{Polymer}} - \rho_{\text{Li (100)}} \quad (2)$$

where $\rho_{\text{Polymer@Li (100)}}$ is the charge density of the interacting system (after optimisation) while ρ_{Polymer} and $\rho_{\text{Li (100)}}$ are the charge densities of the isolated polymer and the Li (100) slab, respectively. The polymer and the Li (100) surface were kept in exactly the same positions as in the final system. The CDDs is thereby correlated to charge depletions and accumulations in the interfacial regions. The 3D CDDs are displayed in Fig. 4 for all oligomers. It can be seen that for PEO (Fig. 4a), PVA (Fig. 4b), and PEI (Fig. 4d), charge accumulation occurs between Li atoms and the lone pairs of the N/O atoms of the oligomers. In the oligomers with ester/carbonate functional groups, i.e. PEC (Fig. 4c), PCL (Fig. 4e), PTMC (Fig. 4f), and in the nitrile group in PAN (Fig. 4g), a different type of charge redistribution is observed in the interfacial region. In these molecules, charge depletion (cyan colour) can be seen in the upper layer of the slab and charge accumulation (yellow), around the O/N functionalities of the polymer. Among all investigated polymers, PAN shows the highest charge redistribution when in contact with the Li metal, indicating strong interactions between the nitrogen atoms and the surface. This is in accordance with the highest adsorption energy of PAN on the surface. PEC and PTMC have the highest redistribution of the charge in the interface after PAN. The trend of the CDDs is clearly corresponding to the trend in adsorption energies. Better adhesion to the surface and greater charge distribution in the interface could protect the surface from other parasitic reactions, and can therefore be considered as important parameters for longer cycle life.[57]

As discussed above, it cannot be straightforwardly concluded that adhesion and charge redistribution are always desired properties. Information about the electronic structure, and also the reactivity of the polymer molecules, is required. Calculation of the DOS can provide information regarding the possibilities of electron transfer across the interface. To investigate the changes in the electronic structure of the oligomers before and after interaction with the Li metal surface, the atomic projected DOS are shown in Fig. 4. Two DOS are computed, one for the molecule further from the surface (without interaction but yet

being placed in the same supercell as the Li metal slab) and one for the molecule interacting with the Li metal surface. This approach allows us to investigate how the electronic structure changes following adsorption. After adsorption, a broadening of the LUMO of the oligomers can be observed with a shift to lower energy levels, moving close to the Fermi level. The reduction in the HOMO–LUMO gap (HLG) of some oligomers and the downward shift of the LUMO to the Fermi level, corresponds to a reduction in the barrier for electron transfer from Li metal to the polymer (lower Schottky barrier). In PEC and PTMC, the HLG becomes much smaller compared to before adsorption, indicating that chances are high for spontaneous redox reactions which can ultimately decompose the macromolecules. The LUMO for PCL is also fairly close to the Fermi level, suggesting that also the polyester can react easy with the Li metal. For PAN, a metallisation clearly occurs upon adsorption, strongly indicating that a rapid electron injection into the oligomer is very likely.

PEO, PVA and PEI, on the other hand, can be considered much better insulating comparing to PEC, PTMC, PCL and PAN based on the DOS plots, and could therefore intuitively be considered as better SPE or coating candidates. These results are, however, based on the crude approximation of only studying one comparatively short chain on the surface, while the entire surface would be covered in a realistic system. It should also be kept in mind that the passivating properties of the different oligomers are highly dependent on the nature of the decomposition products. If these are electronically insulating, ionically conducting, and possess a strong adhesion, a robust SEI layer is formed.

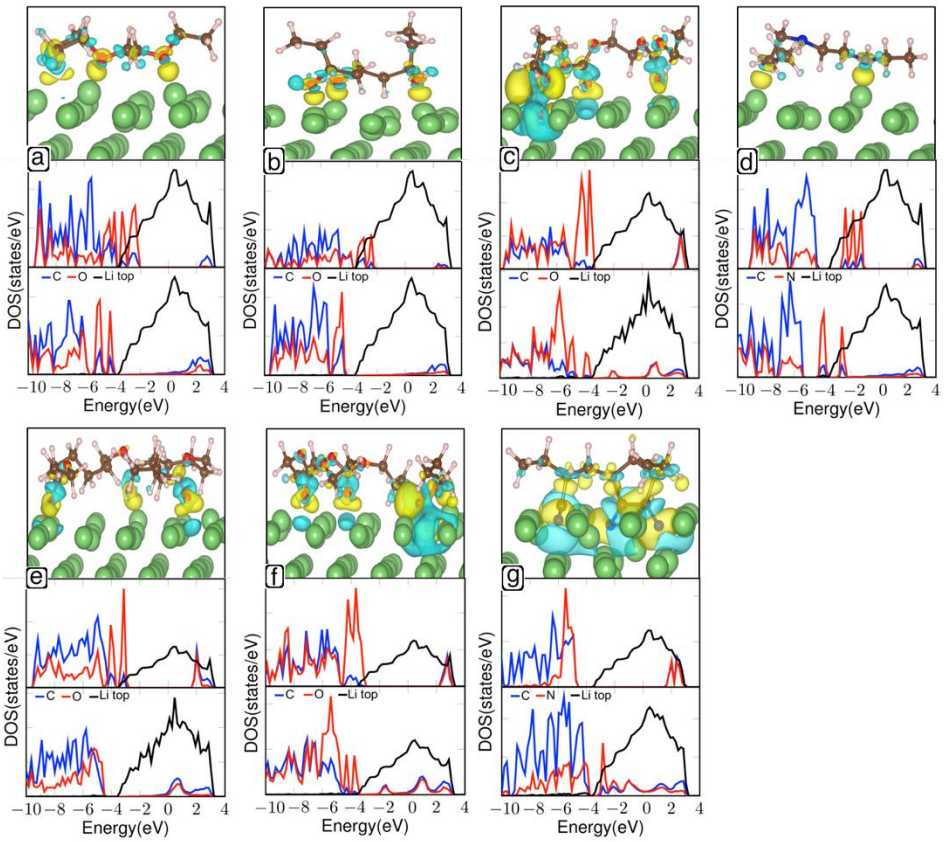

Fig. 4. Side view of 3D charge density differences and density of states plots of (a) PEO (b) PVA (c) PEC (d) PEI (e) PCL (f) PTMC (g) PAN on the Li (100) slab. The yellow (positive region) and cyan (negative region) colours represent the charge accumulation and the charge depletion, respectively. The iso-surface value was set to 0.003 a_0^{-3} (a_0 being the Bohr radius). In the DOS plots, the top part corresponds to the molecule being far from the surface (non-interacting), while the bottom part corresponds to the molecule being in close contact with the surface. Fermi level is set to 0 eV.

3.3 Polymer decompositions on the Li metal surface

In this section, the early-stage interactions of the polymeric molecules with the Li metal surface are explored by means of AIMD simulations for 15 ps at 400 K. The molecules were placed randomly on the surface within around 2–3 Å distance from the upper Li layer in the beginning of the simulations. The final snapshots of the polymer/Li metal structure are shown in Fig. 5.

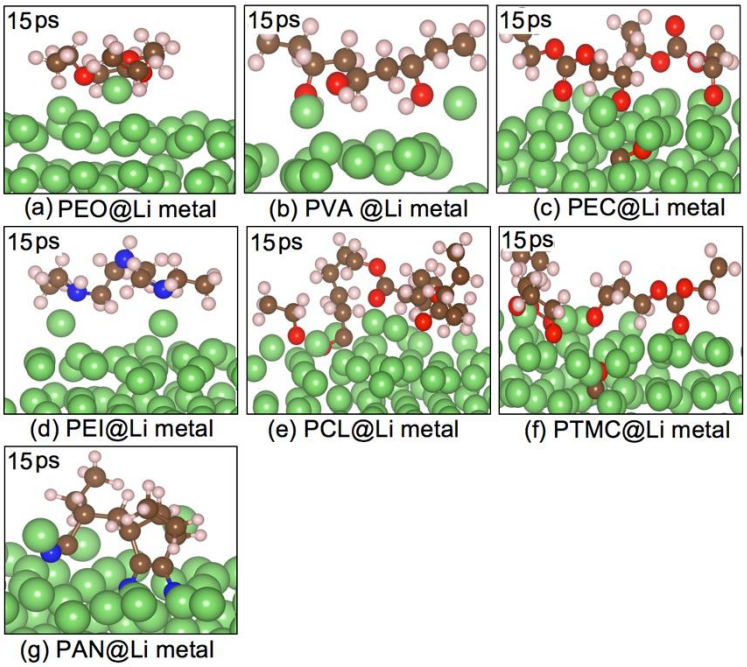

Fig. 5. The final snapshots of AIMD simulations after 15 ps for (a) PEO (b) PVA (c) PEC (d) PEI (e) PCL (f) PTMC (g) PAN at the Li (100) slab at 400 K.

PEO (Fig. 5a) does not undergo any bond cleavage and remains stable during the full length of the simulation time, while Li atoms move up from the surface towards the ether oxygens of PEO. It has been reported that some high-molecular-weight polymers, such as PEO, are thermodynamically stable with Li even at elevated temperatures, indicating no or limited reactions between PEO and the Li metal.[58] On the other hand, experimentally studied PEO electrolyte/Li metal interfaces using X-ray photoelectron spectroscopy (XPS), could detect significant amounts of alkoxide species from degradation of PEO, but these results could also be influenced by high amounts of water residuals in the samples.[36]

Fig. 5b displays the case of PVA. Although there are interactions between O of the alcoholic groups in the oligomer and the Li atoms, no obvious bond breaking occurs, and surprisingly also the hydrogen in the OH groups, which should be fairly acidic, remains bonded to the oligomer.

The carbonate PEC oligomer, on the other hand, undergoes $C_{carbonyl}$–$O_{ethereal}$ bond breakings, producing CO and alkoxides. As can be seen in Fig. 5c, the CO fragment diffused to the surface of the Li metal. The possibility of producing gaseous molecules such as CO or CO_2 from the decomposition of the solid polymer electrolytes (and the difficulty of detecting them by spectroscopic methods) have been discussed in experimental studies, where it has been suggested that the gas molecules mostly dissolve into the SPE.[35] Similar decomposition of cyclic and linear low-molecular-weight carbonates have also been predicted in previous computational works.[44,59]

Simulations of PEI at the Li metal (Fig. 5d) surface does not show any bond breaking during the simulation time. The N atoms instead pull Li atoms from the surface, indicating an atomic complexation rather than a redox reaction. PCL interacts with Li metal through a molecular bond-breaking pathway, similar as for PEC via a $C_{carbonyl}$–$O_{ethereal}$ bond cleavage, but here producing only alkoxide species. It can be seen in Fig. 5e that within the 15 ps simulation time, only one of the three C–$O_{ethereal}$ bonds in PCL is broken. In the other two ester functionalities of the molecule, the $O_{carbonyl}$ interact with the Li atom of the surface.

Fig. 5f shows the results of the simulation of PTMC. Interestingly, this molecule decomposed over the simulation time similarly to PEC, and thereby generated both alkoxide and CO molecules. The possible decomposition pathways for PTMC electrolytes during reduction at a graphite or Li metal interface have been discussed by Sun *et al.,*[35] and one of the proposed pathways is very similar to the obtained fragments here.

In Fig. 5g, the interaction of PAN with Li (100) is presented. The input for the AIMD simulation of PAN is the optimised structure from the energy minimisation process. To investigate also other possibilities, a starting point with a more linear structure of PAN was additionally considered for the AIMD simulation. In neither of these simulations could any clear bond breakings be observed during the 15 ps of simulation time, although some bond distances changed slightly. This is somewhat surprising, and in stark contrast to experimental observations,[60] but could be related to that PAN (and likewise PVA) does not have any heteroatoms in its backbone, and it could therefore be expected that fragmentation is more difficult, requiring longer simulations times. The higher temperature, 600 K, has been considered to see if it could

lead to additional bond breakings in the polymers. The AIMD simulations at this temperature were performed for the three polymers PAN, PVA and PEO. However, the results were the same as for 400 K.

In conclusion, the results of the AIMD simulations for PEC, PTMC and PCL clarify that the strong adhesion of these molecules to the surface indeed leads to a higher reactivity of these molecules on the surface, while PAN constitutes somewhat of an anomaly when compared to the calculated DOS (Fig. 4).

To get better insight into the decomposition process of these three reactive polymers – PEC, PCL and PTMC – possible decomposition pathways were proposed and studied in detail through DFT calculations. The carbonate-based polymers are in many ways analogous to liquid organic carbonates, and similar pathways can therefore be assumed; *i.e.* through $C_{carbonyl}$–$O_{ethereal}$ and $C_{ethereal}$–$O_{ethereal}$ bond breakings.[44] For PEC and PTMC (the two carbonate-based polymers), two decomposition pathways were considered by breaking one of these bonds as a starting point. These two possible bond cleavages are shown in Fig. 6a and b for PTMC and Fig. 6c and d for PEC, respectively. For PCL, only the $C_{carbonyl}$–$O_{ethereal}$ bond breaking was considered and is presented in Fig. 6e. DOS plots of the decomposed polymers are also displayed in Fig. 6 for each pathway.

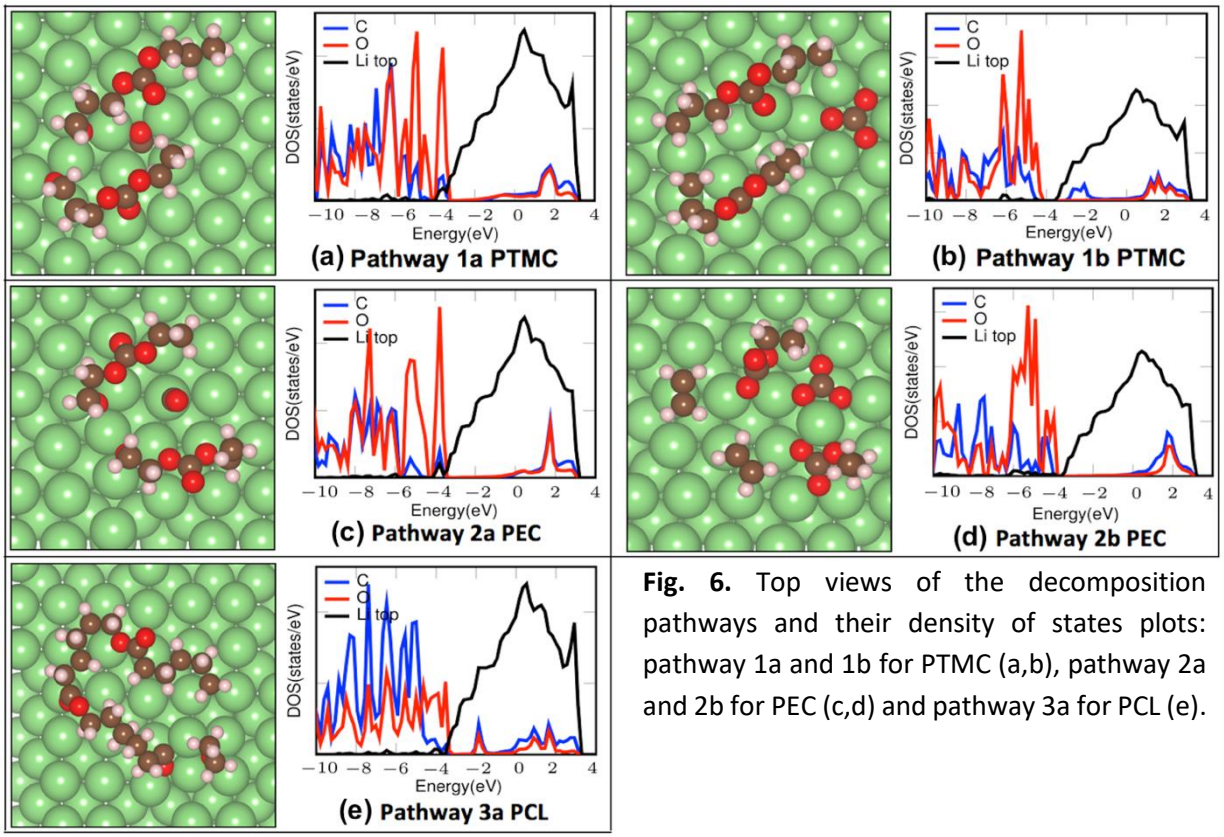

Fig. 6. Top views of the decomposition pathways and their density of states plots: pathway 1a and 1b for PTMC (a,b), pathway 2a and 2b for PEC (c,d) and pathway 3a for PCL (e).

Fig. 6a shows the CO-producing pathway for PTMC. In this pathway, CO diffused to the Li surface after relaxation. The bond distance of this C–O species was 1.32 Å, and the C part of the molecule was facing the surface. The projected DOS plot of this pathway is displayed in Fig. 6a and indicates that there is coupling between the polymer fragments and the Li metal. The alternative carbonate (CO_3^{2-})-producing pathway for PTMC is shown in Fig. 6b. The free carbonate ion was adsorbed to the Li surface upon relaxation, and each O atom of the ion binds to three adjacent Li atoms of the surface. Both alkoxide and alkyl carbonate are reported as common SEI components in XPS measurements of PTMC-based SPEs.[35] Moreover, and in contrast to the products of the pathway in Fig. 6a, the atomic projected DOS for the products of this pathway displays a gap between the HOMO and LUMO, which indicates insulating – and thereby passivating – properties, which are of importance for the stabilisation of the interface.

Pathway 2a of PEC decomposition can be seen in Fig. 6c. Similar to PTMC, the CO molecule is here adsorbed on the surface with the C head towards the Li slab. The bond distance of this molecule is 1.17 Å after relaxation. The DOS plot in Fig. 6c shows that the Fermi level is in the proximity of the LUMO,

indicating a low barrier for electron transfer from the surface to the LUMO of the polymer. The HLG of the PEC products shown in the DOS plot for pathway b (Fig. 6d) is slightly larger than for pathway a, again indicating that the pathway b fragments are better insulating the surface. The HLG for the products of this pathway is also higher than the one in pathway b of PTMC (Fig. 6b), at first sight suggesting slightly more preferable passivating properties for PEC. Interestingly, however, the polymeric molecule formed from pathway b for PEC (Fig. 6d) decomposed further upon relaxation and also produced two free ethylene molecules with an average C–C bond distance of 1.35 Å. Finally, Fig. 6e displays the optimised structure and DOS of decomposed PCL. In PCL, the LUMO is, similar to pathway a of PTMC and PEC, in the proximity of the Fermi level. This is likely related to that the decomposition products are similar in all cases.

Based on the calculated DOS, carbonate products from the decompositions of PEC and PTMC, could indeed form an insulating layer based on their comparatively large HLGs. Carbonate fragments are also widely reported[61,62]as a component of the SEI layer in the Li-metal batteries. The alkoxide fragments from PEC, PTMC and PCL, however, have a smaller HLG and thus seem to be weaker in the formation of an insulating layer.

The energy of the decomposition of the polymeric molecules have been calculated from the difference (ΔE) between the energy of the intact molecule at the surface and the energy of the decomposed counterparts on the Li surface. These energies are reported for each pathway in Fig. 7. For both PTMC and PEC, decomposition pathway b is favoured; *i.e.* through formation of carbonate ions. Pathway b is 0.96 eV more favourable than pathway a in PTMC while for PEC, pathway b is significantly more favourable (by 6.07 eV) than pathway a. The subsequent bond breakings upon relaxation in the PEC – which produce free ethylene molecules – are likely the reason for this large difference between the energies of the two pathways for this polymer. Based on the energetics of the suggested degradation pathways, PCL displays the lowest probability of decomposition of these polymers.

The favourable energetics in the formation of the fragments when adsorbed on the surface through pathway b of PEC and PTMC indicate a higher stability of these fragments, which – considering their corresponding HLGs – could serve as a factor controlling parasitic reactions between the electrolyte and

the electrode in a battery cell. Since the products of pathway b are better-insulating, as discussed above, together with the good adhesion of the produced fragments, highlights that the carbonate-containing fragments of these polymers should be able to provide a favourable SEI layer on the surface of Li metal.

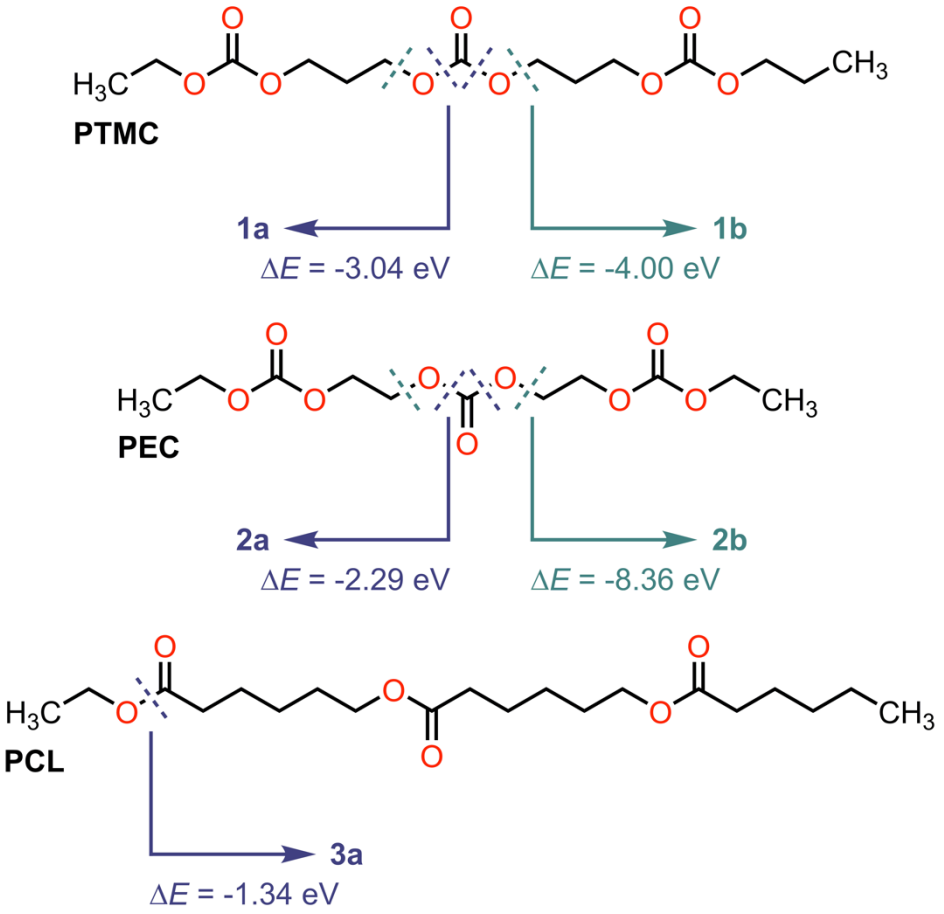

Fig. 7. Decomposition energy for degradation of PTMC, PEC and PCL at the Li metal surface.

Conclusions

Molecular modelling studies of oligomeric molecules with ion-coordinating motifs have been performed at the surface of Li (100) metal in order to get insight into the atomistic interactions between the polymers and the metal surface. This is a first step towards a better understanding of polymer decomposition, polymer film adhesion and SEI formation processes at these important interfaces in Li-metal batteries.

The DFT results show that the polymeric molecules with ester, carbonate and nitrile functional groups adhere more strongly to the surface and display a high charge redistribution, showing that these polymers have considerable differences in their surface chemistry with Li metal as compared to polyethers,

polyamines and polyalcohols. The frontier orbitals in the DOS also show a less insulating pattern for PEC, PTMC and PCL, and a completely metallic system for PAN on the surface, while PEO, PEI and PVA showed rather promising insulating capabilities. Consequently, the carbonate and ester groups undergo rapid bond cleavage as compared to the other ion-coordinating motifs. Therefore, the strong adhesion and the higher charge redistribution for the ester-based oligomers at the surface of the Li metal also correspond to a higher reactivity at the surface. This indicates that these strongly adhesive polymers are less useful when applied to Li metal, if not their decomposition products possess ion-conductive and passivating properties.

Further refinements were therefore done to analyse the energetics of the polymer decomposition mechanisms. Through DFT calculations, it could be seen that the $C_{ethereal}$–$O_{ethereal}$ bond cleavage in the carbonate-containing oligomers was thermodynamically more favourable, while primarily $C_{carbonyl}$–$O_{ethereal}$ bond breaking occurred in the AIMD simulations. These differences indicate that while the former decomposition is thermodynamically favourable, the latter is kinetically preferred. Interestingly, the DOS of the products of the carbonate-producing pathway was found to be better-insulating compared to the alkoxide-producing pathway, while their formation is also energetically favourable. These results suggest that carbonate containing fragments are likely components of the inner part of SEI, and that also the polycarbonates and polyesters can serve as promising SPE hosts, despite some unavoidable decomposition.

While these results give important information about the thermodynamic preconditions for the stability of polymer electrolyte host materials on Li meal electrodes, future studies should also consider the salt component of the electrolytes for a more realistic picture of the electrolyte system and to explore how the interplay between its constituents affects the interfacial chemistry. Yet another important step is to directly correlate the computational results to experimental counterparts, e.g. XPS data, to obtain better refined models.[63] It is also highly relevant to further investigate the properties of the electrolyte decomposition products and their interactions with Li metal, not merely the polymer stability. If the decomposed polymer/salt complexes possess the desired properties of ionic conductivity and surface passivation, also less stable electrolytes will be useful in Li-metal battery systems.

Conflicts of interest

There are no conflicts to declare.

Acknowledgements

This project was supported by the Swedish Energy Agency grant number 39036-1, STandUP for Energy, the Carl Trygger Foundation, the Swedish Research Council (VR) (grant number: 621-2014-5984) and has also been financed through the European Research Council, grant no. 771777 'FUN POLYSTORE'. The computations were carried out on resources provided by the Swedish National Infrastructure for Computing (SNIC) at the NSC and PDC Center for High Performance Computing.

References

1 K. Xu, Electrolytes and Interphases in Li-Ion Batteries and Beyond, *Chem. Rev.*, 2014, **114**, 11503–11618.

2 D. E. . Fenton, J. M. . Parker and P. V. Wright, Complexes of alkali metal ions with poly(ethylene oxide), *Polymer (Guildf).*, 1973, **14**, 589.

3 P. V. Wright, Electrical conductivity in ionic complexes of poly(ethylene oxide), *Br. Polym. J.*, 1975, **7**, 319.

4 X. Yu and A. Manthiram, Electrode-Electrolyte Interfaces in Lithium-based Batteries, *Energy Environ. Sci.*, 2018, **11**, 527–543.

5 M. B. Armand, J. M. Chabagno and M. Duclot, in *Second International Meeting on Solid Electrolytes*, 1978.

6 W. Xu, J. Wang, F. Ding, X. Chen, E. Nasybulin, Y. Zhang and J.-G. Zhang, Lithium metal anodes for rechargeable batteries, *Energy Environ. Sci.*, 2014, **7**, 513–537.

7 J. Mindemark, M. J. Lacey, T. Bowden and D. Brandell, Beyond PEO—Alternative host materials for Li+-conducting solid polymer electrolytes, *Prog. Polym. Sci.*, 2018, **81**, 114–143.

8 Y. Tominaga, V. Nanthana and D. Tohyama, Ionic conduction in poly(ethylene carbonate)-based rubbery electrolytes including lithium salts, *Polym. J.*, 2012, **44**, 1155–1158.

9 M. M. Silva, S. C. Barros, M. J. Smith and J. R. MacCallum, Characterization of solid polymer electrolytes based on poly(trimethylenecarbonate) and lithium tetrafluoroborate, *Electrochim. Acta*, 2004, **49**, 1887–1891.

10 M. Manuela Silva, P. Barbosa, A. Evans and M. J. Smith, Novel solid polymer electrolytes based on poly(trimethylene carbonate) and lithium hexafluoroantimonate, *Solid State Sci.*, 2006, **8**, 1318–1321.

11 T. Okumura and S. Nishimura, Lithium ion conductive properties of aliphatic polycarbonate, *Solid State Ionics*, 2014, **267**, 68–73.

12 J. Mindemark, B. Sun and D. Brandell, Hydroxyl-functionalized poly(trimethylene carbonate) electrolytes for 3D-electrode configurations, *Polym. Chem.*, 2015, **6**, 4766–4774.

13 J. Mindemark, B. Sun, E. Törmä and D. Brandell, High-performance solid polymer electrolytes for lithium batteries operational at ambient temperature, *J. Power Sources*, 2015, **298**, 166–170.

14 Y. M. Lee, N. S. Choi, J. H. Park and J. K. Park, Electrochemical performance of lithium/sulfur batteries with protected Li anodes, *J. Power Sources*, 2003, **119**–**121**, 964–972.

15 H. Lee, D. J. Lee, Y. J. Kim, J. K. Park and H. T. Kim, A simple composite protective layer coating that enhances the cycling stability of lithium metal batteries, *J. Power Sources*, 2015, **284**, 103–108.

16 X. Zhang, Q. Zhang, X. G. Wang, C. Wang, Y. N. Chen, Z. Xie and Z. Zhou, An Extremely Simple Method for Protecting Lithium Anodes in Li-O2 Batteries, *Angew. Chemie - Int. Ed.*, , DOI:10.1002/anie.201807985.

17 P. Johansson, Electrochimica Acta Computational modelling of polymer electrolytes : What do 30 years of research efforts provide us today ?, *Electrochim. Acta*, 2015, **175**, 42–46.

18 G. D. Smith and O. Borodin, in *Batteries for Sustainability*, Springer, New York, NY, 2013.

19 T. F. Miller, Z. Wang, W. Coates and N. P. Balsara, Designing Polymer Electrolytes for Safe and High Capacity Rechargeable Lithium Batteries, *Acc. Chem. Res.*, 2017, **50**, 590–593.

20 M. A. Webb, Y. Jung, D. M. Pesko, B. M. Savoie, U. Yamamoto, G. W. Coates, N. P. Balsara, Z. G. Wang and T. F. Miller, Systematic computational and experimental investigation of lithium-ion transport mechanisms in polyester-based polymer electrolytes, *ACS Cent. Sci.*, 2015, **1**, 198–205.

21 B. Sun, J. Mindemark, E. V. Morozov, L. T. Costa, M. Bergman, P. Johansson, Y. Fang, I. Furó and D.

Brandell, Ion transport in polycarbonate based solid polymer electrolytes: Experimental and computational investigations, *Phys. Chem. Chem. Phys.*, 2016, **18**, 9504–9513.

22 N. D. Lepley, N. A. W. Holzwarth and Y. A. Du, Structures, Li+ mobilities, and interfacial properties of solid electrolytes Li3PS4 and Li3PO4 from first principles, *Phys. Rev. B - Condens. Matter Mater. Phys.*, 2013, **88**, 21–23.

23 T. Cheng, B. V. Merinov, S. Morozov and W. A. Goddard, Quantum Mechanics Reactive Dynamics Study of Solid Li-Electrode/Li6PS5Cl-Electrolyte Interface, *ACS Energy Lett.*, 2017, **2**, 1454–1459.

24 M. Sumita, Y. Tanaka, M. Ikeda and T. Ohno, Theoretically designed li3PO4(100)/LiFePO4(010) coherent electrolyte/cathode interface for all solid-state li ion secondary batteries, *J. Phys. Chem. C*, 2015, **119**, 14–22.

25 J. Haruyama, K. Sodeyama, L. Han, K. Takada and Y. Tateyama, Space-charge layer effect at interface between oxide cathode and sulfide electrolyte in all-solid-state lithium-ion battery, *Chem. Mater.*, 2014, **26**, 4248–4255.

26 J. Haruyama, K. Sodeyama and Y. Tateyama, Cation Mixing Properties toward Co Diffusion at the LiCoO 2 Cathode/Sulfide Electrolyte Interface in a Solid-State Battery, *ACS Appl. Mater. Interfaces*, 2017, **9**, 286–292.

27 M. Sumita, Y. Tanaka, M. Ikeda and T. Ohno, Charged and Discharged States of Cathode/Sulfide Electrolyte Interfaces in All-Solid-State Lithium Ion Batteries, *J. Phys. Chem. C*, 2016, **120**, 13332–13339.

28 W. D. Richards, L. J. Miara, Y. Wang, J. C. Kim and G. Ceder, Interface Stability in Solid-State Batteries, *Chem. Mater.*, 2016, **28**, 266–273.

29 S. Wenzel, S. Randau, T. Leichtweiß, D. A. Weber, J. Sann, W. G. Zeier and J. Janek, Direct Observation of the Interfacial Instability of the Fast Ionic Conductor Li10GeP2S12 at the Lithium Metal Anode, *Chem. Mater.*, 2016, **28**, 2400–2407.

30 Y. Zhu, X. He and Y. Mo, Origin of Outstanding Stability in the Lithium Solid Electrolyte Materials: Insights from Thermodynamic Analyses Based on First-Principles Calculations, *ACS Appl. Mater. Interfaces*, 2015, **7**, 23685–23693.

31 Y. Zhu, X. He and Y. Mo, First principles study on electrochemical and chemical stability of solid electrolyte-electrode interfaces in all-solid-state Li-ion batteries, *J. Mater. Chem. A*, 2016, **4**, 3253–3266.

32 A. Aabloo, M. Klintenberg and J. O. Thomas, Molecular dynamics simulation of a polymer-inorganic interface, *Electrochim. Acta*, 2000, **45**, 1425–1429.

33 O. Borodin, G. D. Smith, R. Bandyopadhyaya and O. Byutner, Molecular Dynamics Study of the Influence of Solid Interfaces on Poly(ethylene oxide) Structure and Dynamics, *Macromolecules*, 2003, **36**, 7873–7883.

34 M. Ebadi, L. T. Costa, C. M. Araujo and D. Brandell, Modelling the Polymer Electrolyte/Li-Metal Interface by Molecular Dynamics simulations, *Electrochim. Acta*, 2017, **234**, 43–51.

35 B. Sun, C. Xu, J. Mindemark, T. Gustafsson, K. Edström and D. Brandell, At the polymer electrolyte interfaces: the role of the polymer host in interphase layer formation in Li-batteries, *J. Mater. Chem. A*, 2015, **3**, 13994–14000.

36 C. Xu, B. Sun, T. Gustafsson, K. Edström, D. Brandell and M. Hahlin, Interface layer formation in solid polymer electrolyte lithium batteries: An XPS study, *J. Mater. Chem. A*, 2014, **2**, 7256–7264.

37 P. E. Blöchl, Projector augmented-wave method, *Phys. Rev. B*, 1994, **5**, 17953–17978.

38 G. Kresse and D. Joubert, From ultrasoft pseudopotentials to the projector augmented-wave method, *Phys. Rev. B - Condens. Matter Mater. Phys.*, 1999, **59**, 1758–1775.

39 G. Kresse and J. Furthmüller, Efficient iterative schemes for ab initio total-energy calculations using a plane-wave basis set, *Phys. Rev. B*, 1996, **54**, 11169.

40 J. P. Perdew, K. Burke and M. Ernzerhof, Generalized Gradient Approximation Made Simple, *Phys. Rev. Lett*, 1996, **77**, 3865–3868.

41 H. J. Monkhorst and J. D. Pack, Special points for Brillouin-zone integrations, *Phys. Rev. B*, 1976, **13**, 5188.

42 J. D. Pack and H. J. Monkhorst, 'Special points for Brillouin-zone integrations'—a reply, *Phys. Rev. B*, 1977, **16**, 1748.

43 A. O. Pereira and C. R. Miranda, Atomic scale insights into ethanol oxidation on Pt, Pd and Au metallic nanofilms: A DFT with van der Waals interactions, *Appl. Surf. Sci.*, 2014, **288**, 564–571.

44 M. Ebadi, D. Brandell and C. M. Araujo, Electrolyte decomposition on Li-metal surfaces from first-principles

theory, *J. Chem. Phys.*, 2016, **145**, 204701.

45 M. J. Frisch, G. W. Trucks, H. B. Schlegel, G. E. Scuseria, M. A. Robb, J. R. Cheeseman, G. Scalmani, V. Barone, B. Mennucci, G. A. Petersson, H. Nakatsuji, M. Caricato, X. Li, H. P. Hratchian, A. F. Izmaylov, J. Bloino, G. Zheng and D. J. Sonnenber, *Gaussian, Inc. Wallingford CT*, 2009.

46 W. J. Hehre, K. Ditchfield and J. A. Pople, Self-consistent molecular orbital methods. XII. Further extensions of gaussian-type basis sets for use in molecular orbital studies of organic molecules, *J. Chem. Phys.*, 1972, **56**, 2257–2261.

47 R. Krishnan, J. S. Binkley, R. Seeger and J. A. Pople, Self-consistent molecular orbital methods. XX. A basis set for correlated wave functions, *J. Chem. Phys.*, 1980, **72**, 650–654.

48 A. D. McLean and G. S. Chandler, Contracted Gaussian basis sets for molecular calculations. I. Second row atoms, Z=11-18, *J. Chem. Phys.*, 1980, **72**, 5639–5648.

49 M. M. Francl, W. J. Pietro, W. J. Hehre, J. S. Binkley, M. S. Gordon, D. J. DeFrees and J. A. Pople, Self-consistent molecular orbital methods. XXIII. A polarization-type basis set for second-row elements, *J. Chem. Phys.*, 1982, **77**, 3654–3665.

50 M. J. Frisch, J. A. Pople and J. S. Binkley, Self-consistent molecular orbital methods 25. Supplementary functions for Gaussian basis sets, *J. Chem. Phys.*, 1984, **80**, 3265–3269.

51 Y. Zhao and D. G. Truhlar, The M06 suite of density functionals for main group thermochemistry, thermochemical kinetics, noncovalent interactions, excited states, and transition elements: Two new functionals and systematic testing of four M06-class functionals and 12 other functionals, *Theor. Chem. Acc.*, , DOI:10.1007/s00214-007-0310-x.

52 G. R. Hanwell, M.D., Curtis, D.E., Lonie, D.C., Vandermeersch, T., Zurek, E., Hutchison, Avogadro: an advanced semantic chemical editor, visualization, and analysis platform, *J. Cheminform.*, 2012, **4**, 17.

53 K. Mathew, R. Sundararaman, K. Letchworth-Weaver, T. A. Arias and R. G. Hennig, Implicit solvation model for density-functional study of nanocrystal surfaces and reaction pathways, *J. Chem. Phys.*, , DOI:10.1063/1.4865107.

54 B. K. Wheatle, J. R. Keith, S. Mogurampelly, N. A. Lynd and V. Ganesan, Influence of Dielectric Constant on

Ionic Transport in Polyether-Based Electrolytes, *ACS Macro Lett.*, 2017, **6**, 1362–1367.

55 S. N. Steinmann, C. Michel, R. Schwiedernoch and P. Sautet, Impacts of electrode potentials and solvents on the electroreduction of CO2: A comparison of theoretical approaches, *Phys. Chem. Chem. Phys.*, 2015, **17**, 13949–13963.

56 G. Glockler, Relation between bond energies and bond distances, *J. Phys. Chem.*, 1957, **61**, 31–38.

57 M. Boota, C. Chen, M. Bécuwe, L. Miao and Y. Gogotsi, Pseudocapacitance and excellent cyclability of 2,5-dimethoxy-1,4-benzoquinone on graphene, *Energy Environ. Sci.*, 2016, **9**, 2586–2594.

58 K. Zaghib, M. Armand and M. Gautier, Electrochemistry of Anodes in Solid-State Li-Ion Polymer Batteries, *J. Electrochem. Soc.*, 1998, **145**, 3135–3140.

59 L. E. Camacho-Forero, T. W. Smith, S. Bertolini and P. B. Balbuena, Reactivity at the Lithium-Metal Anode Surface of Lithium-Sulfur Batteries, *J. Phys. Chem. C*, 2015, **119**, 26828–26839.

60 P. Hu, J. Chai, Y. Duan, Z. Liu, G. Cui and L. Chen, Progress in nitrile-based polymer electrolytes for high performance lithium batteries, *J. Mater. Chem. A*, 2016, **4**, 10070–10083.

61 I. Ismail, A. Noda, A. Nishimoto and M. Watanabe, XPS study of lithium surface after contact with lithium-salt doped polymer electrolytes, *Electrochim. Acta*, 2001, **46**, 1595–1603.

62 X.-B. Cheng, R. Zhang, C.-Z. Zhao, F. Wei, J.-G. Zhang and Q. Zhang, A Review of Solid Electrolyte Interphases on Lithium Metal Anode, *Adv. Sci.*, 2015, **3**, 1500213.

63 M. Ebadi, A. Nasser, M. Carboni, R. Younesi, C. F. N. Marchiori, D. Brandell and C. M. Araujo, Insights into the Li-Metal/Organic Carbonate Interfacial Chemistry by Combined First-Principles Theory and X-ray Photoelectron Spectroscopy, *J. Phys. Chem. C*, , DOI:10.1021/acs.jpcc.8b07679.

